

Reactions in flows with nonhyperbolic dynamics

Alessandro P. S. de Moura* and Celso Grebogi

Instituto de Física, Universidade de São Paulo, Caixa Postal 66318, 05315-970, São Paulo, SP, Brazil

(Received 9 April 2003; revised manuscript received 27 May 2004; published 29 September 2004)

We study the reaction dynamics of active particles that are advected passively by 2D incompressible open flows, whose motion is nonhyperbolic. This nonhyperbolicity is associated with the presence of persistent vortices near the wake, wherein fluid is trapped. We show that the fractal equilibrium distribution of the reactants is described by an *effective dimension* d_{eff} , which is a finite resolution approximation to the fractal dimension. Furthermore, d_{eff} depends on the resolution ϵ and on the reaction rate $1/\tau$. As τ is increased, the equilibrium distribution goes through a series of transitions where the effective dimension increases abruptly. These transitions are determined by the complex structure of Cantori surrounding the Kolmogorov-Arnold-Moser (KAM) islands.

DOI: 10.1103/PhysRevE.70.036216

PACS number(s): 47.70.Fw, 83.80.Jx, 47.52.+j

I. BACKGROUND AND MOTIVATION

In this paper we study the dynamics of active processes taking place in a nonstationary open (unbounded) two-dimensional flow. A well-known example is the plane flow incident on a cylindrical obstacle, which is one of the paradigms in fluid mechanics. By “active process” we mean chemical reactions or biological processes, for example. The idea is that particles are advected by the flow and, at the same time, undergo changes due to some internal (intrinsic) dynamics—chemical transformations or biological reproduction, for instance. Instead of talking about particles, one can also describe this process in terms of advected concentration fields of the substances involved. In this case, the dynamics is given by a partial differential equation on the concentrations, coupled to the velocity field of the flow (an *advection-reaction-diffusion equation*). Either way, the overall dynamics of the reactive system depends strongly on the underlying advection dynamics of the flow. In most interesting situations, open flows involving obstacles are expected to generate a chaotic Lagrangian transient dynamics [1]. This means that the motion of a fluid particle typically displays very long transients, during which the motion is chaotic. This is a phenomenon known as chaotic scattering, and it is a generic feature of open flows with obstacles. Chaotic scattering in the flow with a cylindrical obstacle has also been observed experimentally [2]. The question of how this chaotic dynamics affects the reaction dynamics unfolding in the flow has been addressed by a number of previous works [3–5], and many important results have been derived on the relation between the parameters characterizing chaos and the dynamics of the reaction. However, these results have all been obtained by making the assumption that the flow’s chaos is of the simplest kind, namely *hyperbolic*. This means that the flow is assumed to be unstable everywhere. It is known, however, that many (maybe most) flows found experimentally are nonhyperbolic, showing stable regions which correspond to the presence of trapped vortices. The previous

theory does not encompass this more general kind of flow. The aim of this work is to address this issue. We will see that there are many new phenomena due to nonhyperbolicity having no counterpart in hyperbolic flows. The moral is that nonhyperbolicity cannot be neglected if one wants to understand the dynamics of real flows.

The dynamics of chemical and biological activity taking place in nonstationary flows is of great importance in many areas of fundamental and applied science. Two illustrative examples are the series of complex chemical reactions involved in the depletion of the Earth’s ozone layer, and the population dynamics of plankton in the oceans. In these processes, the intrinsic dynamics of the reactive process is coupled to the dynamics of the fluid by the fact that the reacting substances (chemicals or micro-organisms, for example) are being carried along with the flow. In many cases, the reactants can be considered *passive*, meaning that their velocity at a given point is always equal to the velocity of the flow at that point. In other words, their inertia is negligible. If, furthermore, the reactants are present in low concentrations, and if their reactions do not involve too much heat production, it is usually a good approximation to consider that they do not affect the flow significantly. With these approximations, the reaction dynamics is described by an *advection-reaction-diffusion equation*, which is a partial differential equation for the reactants’ concentrations involving explicitly the fluid velocity field \mathbf{u} .

A particularly important class of reaction is that of *autocatalytic* reactions [6,7], of particular importance to biology [8]. The simplest kind of autocatalytic reaction corresponds to the spontaneous growth of the reactant due to a chain reaction, such as the spreading of a flame, or the growth of a population of micro-organisms by self-replication. A simple model for this process is the advection-reaction-diffusion equation [9]

$$\frac{\partial c}{\partial t} + \mathbf{u} \cdot \nabla c = f(c) + \kappa \nabla^2 c. \quad (1)$$

Here, c denotes the concentration of the autocatalytic reactant, κ is the diffusivity, and $\mathbf{u} = \mathbf{u}(\mathbf{r}, t)$ is the flow’s velocity

*Email address: amoura@if.usp.br

field, which is determined from the Navier-Stokes equation, with the appropriate boundary conditions. The intrinsic dynamics of the reaction is determined by $f(c)$, which is usually a nonlinear function of c .

Since c does not affect the flow dynamics, in this work we consider that the (usually hard) task of solving the Navier-Stokes equation is done, and that the velocity field $\mathbf{u}(\mathbf{r}, t)$ is given. We are interested here in how a nonstationary flow \mathbf{u} affects the overall dynamics of the reaction. We make the simplifying assumption that the flow can be considered two-dimensional (2D), $\mathbf{u}=(u_x(x, y, t), u_y(x, y, t))$. This can be physically justified by the fact that in many important cases this is a good approximation. For example, the large-scale dynamics of the atmosphere and the oceans is approximately 2D, because (among other things) of the stratification caused by the Earth's rotation. Furthermore, in most situations the fluid velocities are much smaller than the speed of sound. In this case, we have a 2D incompressible (viscous) flow. As is well known [10], this kind of flow can be described by means of a stream function $\psi=\psi(x, y, t)$, in terms of which the velocity field is given by $u_x=\partial\psi(x, y, t)/\partial y$; $u_y=-\partial\psi(x, y, t)/\partial x$. As a result of the assumption of negligible inertia, the trajectory $(x(t), y(t))$ of a particle of reactant is the same as that of a fluid particle

$$\dot{x} = \partial\psi(x, y, t)/\partial y; \quad \dot{y} = -\partial\psi(x, y, t)/\partial x. \quad (2)$$

The pair of equations (2) has a Hamiltonian structure, with the stream function ψ playing the role of the Hamiltonian, while x is the coordinate and y is its associated ‘‘momentum.’’ The dynamics of a particle passively carried by the flow is thus equivalent to the dynamics of a generally time-dependent one-degree-of-freedom Hamiltonian system, with a phase space corresponding to the (x, y) physical space. We know that, since the ‘‘Hamiltonian’’ ψ is time dependent, in general the (Lagrangian) dynamics is chaotic. This can be so even for very simple time dependencies. For example, chaotic motion generally ensues if ψ is time periodic with some period T , $\psi(x, y, t)=\psi(x, y, t+T)$.

In this work, we consider *open* flows, such as the paradigmatic channel flow with a cylindrical obstacle. In open flows, there are unbounded trajectories, corresponding to particles that come from the upstream region, stay in the wake for a while, and then leave downstream. We notice that even flows which are in reality confined can be considered open if the time it takes for a typical particle to return near the obstacle is much greater than the other relevant time scales. Thus, we can consider the flow of the ocean around an isolated island as an open flow, even though the ocean as a whole is of course bounded. Such 2D open flows model important environmental flows in the atmosphere and in the ocean [11,12].

Equations (2) describe a *scattering* dynamics. There is a bounded region in space, near the wake, in which the dynamics of fluid particles is nontrivial. This is the *interaction region*, or *mixing region*. Outside this region, the velocity field is (approximately) stationary, and the particles follow simple trajectories. Typically, an advected particle comes from the upstream region, enters the mixing region, moves around in

there in a possibly complicated trajectory, and finally leaves towards the downstream region. This transient dynamics is chaotic if the scattering process is very sensitive to initial conditions. Thus, small changes in (for example) the position of the particle before entering the mixing region can affect the final state of the particle tremendously after scattering (that is, after leaving the mixing region). This phenomenon is called *chaotic scattering*, and it is very common in dynamical systems with transients [13,14]. The stream function of typical open flows is likely to display chaotic scattering.

Chaotic scattering is associated with the presence in the mixing region of a highly complex set of nonescaping orbits, the *chaotic saddle*. This set is composed of orbits that never leave the mixing region, for $t\rightarrow\infty$ and $t\rightarrow-\infty$. The chaotic saddle is a fractal set in phase space, with nonsmooth structure on arbitrarily small scales. The *stable* and *unstable manifolds* of the chaotic saddle are the sets of initial conditions which tend to the chaotic saddle as $t\rightarrow\infty$ and $t\rightarrow-\infty$, respectively. Initial conditions on the stable manifold never leave the mixing region after having entered it, and correspond to orbits with a diverging escape time. Because phase space is contracted by time evolution along the stable manifold, and expanded along the unstable manifold, advected particles leave the mixing region near the unstable manifold. Therefore, an open set of initial conditions (corresponding physically to a cloud of advected particles) traces out the unstable manifold after being scattered. The fractal structure of these sets is thus directly observable, and their fractal dimension is a quantitative measure of the sensitivity of the dynamics to the initial conditions.

The simplest nontrivial flow dynamics is for a periodic time dependence of ψ , with $\psi(x, y, t)=\psi(x, y, t+T)$, where T is the period. In this case, the dynamics of an advected particle can be described by a stroboscopic two-dimensional discrete map \mathcal{M} given by

$$\mathcal{M}(x, y) = (x_T, y_T), \quad (3)$$

where (x_T, y_T) is the position of the particle given by the forward integration of Eqs. (2) for a time interval T , for an initial condition $(x_0, y_0)=(x, y)$. Time periodicity arises naturally in open flows. In the case of a cylindrical obstacle, the flow becomes periodic above a critical Reynolds number R_c , at which the steady regime becomes unstable. Although the details may vary, the loss of stability of the steady flow to a periodic flow is a very common phenomenon in open flows, so our theory has a wide range of applicability. Given that the flow is periodic, the reduction of the dynamics to the map \mathcal{M} in (3) is completely general for two-dimensional incompressible (viscous) flows. We note that \mathcal{M} preserves the area, and is thus a *symplectic* map.

The simplest kind of chaotic scattering is *hyperbolic*. In the hyperbolic case, all orbits in the chaotic saddle are unstable, meaning that initial conditions starting arbitrarily close to one of these orbits lead to trajectories that separate exponentially from it, eventually escaping the mixing region. The hyperbolic assumption simplifies the analysis considerably, but it excludes the possibility of stable (elliptic) orbits, which are generic for Hamiltonian systems (and symplectic maps). The dynamics of chemical reactions and other active

processes has been extensively investigated in chaotic open flows, under the assumption that the chaotic saddle is hyperbolic [3,4]. In the case of autocatalytic reactions, after a transient time, the reacting particles settle down to an equilibrium distribution in space which is concentrated around the unstable manifold of the chaotic saddle. The equilibrium distribution can be regarded as a fattened-up version of the unstable manifold, with an average thickness which depends on the reaction rate and on the advection dynamics (see Sec. II for details). In particular, the observed fractal dimension of the reactants is the same as the dimension of the unstable manifold. Moreover, the fractal structure of the chaotic saddle accelerates the reaction and acts as a dynamic catalyst, due to the large surface-volume ratio of the equilibrium distribution, which is a result of its fractal structure. This dynamical catalysis manifests itself as a singular production term in the equation for the reaction rate. Some examples of issues that can be studied within this framework are the depletion of ozone in the polar stratosphere [15], plankton population dynamics on the sea surface [16], and even the origin of life [17].

All the results mentioned above have been obtained for the case when the dynamics of the advected particles is hyperbolic. However, in general Hamiltonian systems are nonhyperbolic, having stable (elliptic) periodic orbits which are surrounded by Kolmogorov-Arnold-Moser (KAM) tori of quasiperiodic orbits, making up *KAM islands* in phase space. No orbit starting from the outside can enter a KAM island, and the fluid in one island never leaves. In fluid mechanical terms, the KAM islands correspond to trapping vortices in the flow. Such vortices are very common in 2D flows, and they have been observed in environmental flows, such as in the atmosphere (the stratospheric polar vortex, which plays a crucial role in the process of ozone depletion [11]), and also in ocean circulation [12]. In this article, we study the dynamics of reactions when the advection dynamics of the particles is nonhyperbolic. We shall see that striking new effects take place because of nonhyperbolicity, and since, as we mentioned above, many important flows are expected to be nonhyperbolic, we expect our results to be relevant for understanding realistic systems.

The rest of this paper is organized as follows. We first investigate the importance of diffusion in the reaction dynamics, and derive the condition under which it can be neglected (Sec. II). We show that in most cases we can neglect diffusion, and consider only advection (along with the reaction itself). We apply our condition to the Fischer autocatalytic reaction, as an example. Next (Sec. III), we introduce a simple 2D symplectic map we use throughout the paper, and we review briefly the relevant concepts about the phase-space structure of nonhyperbolic Hamiltonian systems. In Sec. IV, we introduce the concept of and define what we call the *effective fractal dimension* $d_{eff}(\epsilon)$ for a general Hamiltonian system, which can in particular be applied to 2D incompressible flows. Here, d_{eff} is an approximation of the fractal dimension d of the stable (and unstable) manifold of the chaotic saddle of an open system, for a finite resolution ϵ . We show that d_{eff} is a very important quantity for nonhyperbolic systems in general, and in particular for 2D flows with vortices. It turns out that the effective dimension d_{eff} is of

fundamental importance for understanding the dynamics of reactions taking place in these flows. For a finite lower scale ϵ , d_{eff} is equal to d in the limit as $\epsilon \rightarrow 0$. For nonhyperbolic systems, it is known that $d = d_{ph}$, where d_{ph} is the phase-space dimension [18] (in our case $d=2$). In nonhyperbolic systems, the convergence of d_{eff} to $d = d_{ph}$ as $\epsilon \rightarrow 0$ is very slow, and we show that $d_{eff}(\epsilon)$ is the relevant physical quantity for a finite resolution ϵ . We further show that d_{eff} depends not only on the minimum scale ϵ , but also on the location in phase space. This dependence arises because of the presence of a complex structure of Cantori surrounding the KAM islands. In Sec. V, we investigate the consequences of these results for the dynamics of reactions taking place in the flow. We argue that, since the reaction introduces naturally a lower scale ϵ in the dynamics, the observed dimension of the filamentary structure of the equilibrium distribution of the particles is $d_{eff}(\epsilon)$, and not the true fractal dimension $d=2$. The reaction also introduces a new time scale τ in the dynamics, given by the inverse of the reaction rate. We show that, as a consequence, the observed dimension of the particles' equilibrium distribution depends on τ . As τ is increased, the equilibrium distribution undergoes a series of metamorphoses where the observed dimension increases. We test our theory with a particular system and with a particular kind of reaction (catalysis), but our results are valid in general. These results show that the nonhyperbolic dynamics results in a reaction dynamics that is fundamentally different from the hyperbolic case.

II. REACTION AND DIFFUSION

In this section we define our reaction model, and we investigate the influence of the diffusion, and under what conditions it can be neglected [27].

From now on, we will consider only autocatalytic reactions. A particularly simple autocatalytic reaction is described by a single (suitably normalized) scalar concentration field $c = c(\mathbf{r}, t)$. We assume that the intrinsic chemical dynamics is such that c has two equilibrium values, one of them being stable and the other one being unstable. Without loss of generality, we take $c=0$ to be the unstable value, and $c=1$ to be the stable one. Consider now a stationary fluid ($\mathbf{u}=0$), with initially $c(\mathbf{r}, 0)=0$ throughout the fluid. If we introduce a localized "chemical perturbation" by making $c \neq 0$ in some region, c will clearly tend to the stable value 1 in that region. If there is a spatial coupling, such as the Laplacian term in Eq. (1), the concentration in neighboring points will also move towards 1. As a result, the initial perturbation will propagate, and will end up changing all the fluid to $c=1$ (if it is at rest). If the time scale of the reaction is fast enough, there is an abrupt boundary between the stable ($c \approx 1$) and unstable ($c \approx 0$) regions, with only a negligible region with intermediate values of c . In other words, the stable regions "invade" the unstable regions, much like an infection, in a well-defined front, similar to a shock front. This reaction front propagates with a constant velocity v which depends on properties of the fluid and on details of the reaction.

A very important example of an autocatalytic reaction of this type is given by Fischer’s reaction-diffusion equation [8,19,20]

$$\frac{\partial c}{\partial t} = kc(1 - c) + D\nabla^2 c, \tag{4}$$

where k is the reaction rate, and D is the diffusivity of c . This equation is valid for a stationary flow. Without the diffusion term, Eq. (4) is just the logistic (Verhulst) growth equation. The Fischer equation is then seen to be the model for a “population” which grows locally by the familiar logistic law, and is coupled spatially by diffusion. Equation (4) is the simplest possible generalization of the logistic growth model to include spatial effects. It has been extensively studied due to its importance in biology, and it has been shown that its reaction front velocity is given by

$$v = 2\sqrt{kD}. \tag{5}$$

We now ask what happens when the flow is nonstationary, and moreover when the flow is open. In this case, it is no longer true that the stable “phase” $c=1$ will invade the whole space, as there is competition between the spreading caused by the reaction and the escape caused by advection of the fluid to the downstream region. Rigorously, the dynamics is then given by Eq. (1), with $f(c)=kc(1-c)$. However, we can use the existence of a well-defined reaction front to avoid considering explicitly the convective term in Eq. (1). As the flow moves, both the stable and unstable regions, as well as the boundary separating them, are advected. The boundary is the reaction front, which is spreading from the stable to the unstable regions with velocity v , while, at the same time, it is advected by the flow by Eqs. (2). Hence, the velocity of each point of the front is a result of the composition of the local flow velocity and the intrinsic front velocity v , directed along the normal to the front line (remember, our flow is $2D$). Advection tends to concentrate the particles near the unstable manifold of the chaotic saddle, as we mentioned before. From this we can expect the stable region (c close to 1) of the open time-dependent flow to be concentrated on thin strips around the fractal unstable manifold. If there were no reaction, the width of each strip would contract at a mean rate given by the Lyapunov exponent h (since the flow is Hamiltonian, its positive and negative Lyapunov exponents are equal in modulus), and the total area of the stable region would go to zero, as a result of the escape of flow to the downstream region. The tendency of the front to spread counteracts this shrinking (see Fig. 1).

To model this dynamics, we first consider the simple case without diffusion. Let $\epsilon(t)$ be the average width of the strips containing the stable region. Advection tries to shrink ϵ exponentially, while reaction tries to expand it with a constant speed v . The time-evolution equation for ϵ is then

$$\dot{\epsilon} = -h\epsilon + 2v, \tag{6}$$

where the factor 2 comes from the fact that on each strip the reaction acts on *two* fronts. In equilibrium, we have $\dot{\epsilon}=0$, which using Eq. (6) gives us the equilibrium value ϵ^*

$$\epsilon^* = 2v/h. \tag{7}$$

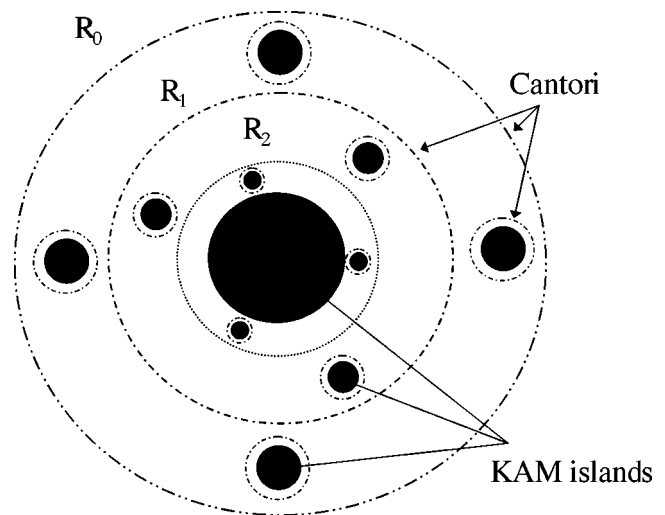


FIG. 1. Schematic illustration of the hierarchical structure of KAM islands and cantori, generic in nonhyperbolic flows. Solid circles represent KAM islands, and cantori are represented by circles with “gaps.”

We now consider the effect of a diffusion D on the above considerations. For a purely diffusive dynamics (without either advection or reaction), each strip would spread as $\epsilon = 2\sqrt{2Dt}$, starting from an infinitesimally thin strip. This time evolution arises from the equation

$$\dot{\epsilon} = \frac{2D}{\epsilon}. \tag{8}$$

Of course, this description of the effect of diffusion as an increase of ϵ given by Eq. (8) is a simplification of the real process. In reality, diffusion causes a continuous spreading of an initial distribution, without sharp boundaries. To simplify our analysis, however, we will continue to work with the strip width ϵ , which is sensible if D is not too large.

Adding Eq. (8) to the right-hand side of Eq. (6), we find the equation for time evolution of the mean strip width due to advection, reaction, and diffusion

$$\dot{\epsilon} = -h\epsilon + \frac{2D}{\epsilon} + 2v. \tag{9}$$

The equilibrium condition $\dot{\epsilon}=0$ gives a quadratic equation for the stationary width ϵ^* . Only the positive solution is physically meaningful

$$\epsilon^* = \frac{v}{h} + \sqrt{\left(\frac{v}{h}\right)^2 + \frac{2D}{h}}. \tag{10}$$

From Eq. (10), we see that the effect of diffusion on the equilibrium width of the strips can be neglected if the second term in the square root is much smaller than the first one, which yields the condition

$$2Dh \ll v^2. \tag{11}$$

This condition involves the parameters characterizing the advection (h), the reaction (v), and the diffusion (D). If (11) is

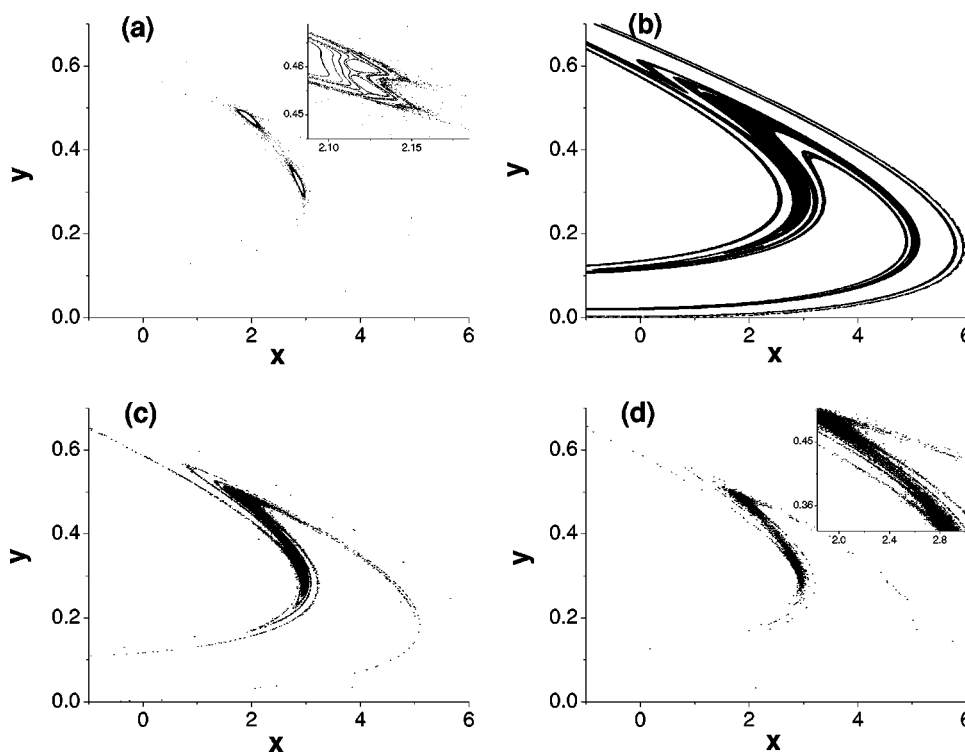


FIG. 2. (a) Orbits of the map (13) for $\lambda=6$. The inset shows a magnification of a small region. Complex structures of stable orbits and Cantori can be seen. (b) Equilibrium distribution for $\lambda=6$ and $\tau=1$; (c) same as (b), with $\tau=50$; (d) same as (b), with $\tau=200$. The magnification in the inset shows the filamentation of the region lying between the two KAM islands.

satisfied, we can forget about the diffusion, and only consider the advection and the reaction.

In general, v depends on D . In the case of Fischer's equation (4), we can use the expression (5) for the front velocity. The condition (11) then becomes

$$h \ll 2k. \quad (12)$$

Surprisingly, D dropped out of the condition. Physically, this happens because the reaction front spreads diffusively in this model, as can be seen by inspecting Eq. (4). Since $1/k$ gives the time scale of the reaction, Eq. (12) implies that (for the Fischer autocatalytic process) diffusion can be safely neglected if the reaction time scale is much shorter than the time scale of separation of nearby trajectories (given by $1/h$).

In what follows, we shall assume that condition (11) [or (12)] is satisfied, and so we do not have to take the diffusion into account. This is known to be true for many important applications, such as the dynamics of the depletion of the ozone layer and the plankton population dynamics.

III. ADVECTION, KAM ISLANDS, CANTORI

We are interested in studying the reaction dynamics in nonhyperbolic flows. We showed in Sec. I that if the flow is time periodic, the advection dynamics is reduced to a discrete-time 2D area-preserving map \mathcal{M} , given by Eq. (3). Since the flows we are interested in are open, \mathcal{M} has unbounded orbits which go to infinity as $t \rightarrow \infty$. The dynamics of \mathcal{M} can be either hyperbolic or nonhyperbolic. In the

former case, all orbits comprising the chaotic saddle are unstable, and the set of nonescaping orbits has null measure (volume). This is the case studied in previous works [3,4]. If the flow is nonhyperbolic, besides the unstable orbits, there are also elliptic orbits with purely imaginary eigenvalues. These orbits are surrounded by KAM islands, complex structures of tori made of quasiperiodic orbits separated by open regions of chaotic motion ("chaotic seas"). Large KAM islands are surrounded by smaller "satellite" islands, which are themselves accompanied by even smaller islands, and so on infinitely. This hierarchical structure of KAM islands, extending through arbitrarily small scales, is depicted in Fig. 1. Besides the islands, there is also a hierarchical structure of Cantori, which are invariant sets with a fractal distribution of gaps (see Fig. 2). One may think of a cantorus as an invariant torus riddled with holes (in a fractal way). Contrary to the invariant tori, particles can cross from one side of a cantorus to the other, although this may take a long time. Cantori act thus as transport barriers. For example, points started in region R_2 in Fig. 2 take on average much longer to escape than those started in region R_1 , and those started in region R_3 take even longer to escape, and so on.

Because of the presence of this structure of KAM islands and cantori, the phase space of nonhyperbolic systems is much more complex than their hyperbolic counterparts, and we shall see that this has important consequences for the reaction dynamics.

From the theory of 2D symplectic maps (Birkhoff's theorem and KAM theory) [21] we know that, although the details may change from system to system, the overall phase-

space structure shown in Fig. 1 is completely general, and shows up in any nonhyperbolic map (and therefore in their associated 2D incompressible flows as well) [21]. This universality allows us to choose a particularly simple nonhyperbolic map as an example, since the results will hold in general. One of the simplest 2D symplectic nonhyperbolic with escapes is [23]

$$\begin{cases} x_{n+1} = \lambda[x_n - (x_n + y_n)^2/4], \\ y_{n+1} = \lambda^{-1}[y_n + (x_n + y_n)^2/4], \end{cases} \quad (13)$$

where λ is a real parameter. The map (13) has an open dynamics, with trajectories coming from infinity, and being scattered towards infinity again after a transient time. For $\lambda \leq 6.5$, the map is nonhyperbolic [18]. We fix $\lambda=6$ throughout this paper. In Fig. 2(a), we show the Poincaré section for this system, found by plotting many iterations of a few initial conditions. There is a stable period-2 orbit, which is the center of a KAM island composed of two pieces. This KAM island is surrounded by a cantorus, which can be seen by the long time it takes for a particle in its interior to escape, as made evident by the outermost orbit, shown in the figure as a cloud of points surrounding the islands. Orbits initialized within the cantorus have an average escape time much larger than those initialized outside it. There are smaller cantori embedded within the big one, corresponding to even larger escape times, and so on, in a hierarchical structure similar to that of the KAM islands themselves [glimpses of this “fine structure” can be seen in the inset of Fig. 2(a)]. We stress again that, although we are looking at the particular case of map (13) for convenience, this self-similar structure of KAM islands and cantori is a general feature of any nonhyperbolic Hamiltonian system.

IV. THE EFFECTIVE FRACTAL DIMENSION

We now introduce the basic concept of effective dimension for the pure (nonreactive) dynamics [22]. In open chaotic systems, the stable (and unstable) manifold of the invariant set is fractal, with the (box-counting) fractal dimension d defined by the limit $d = \lim_{\epsilon \rightarrow 0} \ln N(\epsilon) / \ln(\epsilon^{-1})$, where $N(\epsilon)$ is the number of boxes of size ϵ needed to cover the unstable (or stable) manifold [24,25]. Since for ϵ sufficiently small $N(\epsilon)$ is in most cases a power law, this is equivalent to the limit of the following derivative:

$$d_{ph} - d = \lim_{\epsilon \rightarrow 0} \frac{d \ln f(\epsilon)}{d \ln \epsilon}, \quad (14)$$

where $f(\epsilon)$ is the fraction of boxes of size ϵ needed to cover the fractal set (compared with the total number $\sim \epsilon^{-d_{ph}}$). In general d satisfies $d_{ph} - 1 \leq d \leq d_{ph}$. For nonhyperbolic systems, it is known that d always assumes the maximum value $d = d_{ph}$ ($d_{ph}=2$, in our case). The limit (14), however, converges very slowly and is only attained for *very* small values of ϵ . In fact, in nonhyperbolic systems, a log-log plot of $f(\epsilon)$ versus ϵ is typically, to a very good approximation, a straight line with a nonzero slope over an ϵ range of many orders of magnitude, even though from Eq. (14), the slope is zero for $\epsilon \rightarrow 0$. The slope in fact does approach zero for ϵ small

enough. But, if for some physical reason one has a finite resolution ϵ (given, for instance, by the size of the advected particle, or by the resolution of our viewing apparatus), the dimension that is effectively seen is given by the effective dimension d_{eff} , defined as an approximation to d for finite ϵ

$$2 - d_{eff}(\epsilon) = \left. \frac{d \ln f(\epsilon^*)}{d \ln \epsilon^*} \right|_{\epsilon^*=\epsilon}. \quad (15)$$

We have $d_{ph}=2$ in our case. Obviously, d_{eff} depends on the minimum scale ϵ , and satisfies $d_{eff}(\epsilon) \rightarrow 2$ as $\epsilon \rightarrow 0$ [26].

A most important property of the effective dimension is the following: for nonhyperbolic systems, d_{eff} depends not only on ϵ , but also on the location in phase space. This is due to the presence of cantori in phase space, which act as transport barriers: particles inside a cantorus take a much longer time to escape than those that start outside it. This means that the piece of the chaotic saddle’s stable manifold that is within the cantorus is more stretched and folded than on the outside. At finite resolution, its filamentation appears more involved and, as a result, the effective dimension in the inner region should be higher than in the outer region. We test this idea in the system (13), using the uncertainty method [24] to calculate $f(\epsilon)$, and Eq. (15) to find the effective dimension. We first calculate d_{eff} outside the cantorus, and we find $d_{eff} = 1.54$ [Fig. 3(a), circles]. Inside the first cantorus, we find a considerably greater value $d_{eff} = 1.91$ [Fig. 3(b), circles]. This shows that d_{eff} indeed depends on the location in phase space, and is greater inside a cantorus. We have also verified this result for other systems. There is, however, an infinite number of cantori, organized hierarchically around the KAM islands. As we go deeper and deeper within the cantori structure, the typical escape time increases, and so does d_{eff} . In fact, we were able to find regions in system (13) whose effective dimension is numerically indistinguishable from 2. We point out that, even though in this work we focus mainly on the chemical dynamics, this is a general result, valid for any Hamiltonian system with two degrees of freedom.

V. NONHYPERBOLIC REACTION DYNAMICS

The consequences of the above findings for the reactive dynamics are many and fundamentally relevant. We use autocatalytic reactions as an example, but we expect many of our results to apply more broadly. In order to numerically implement reactions in this system, we perform a discretization of space and time, following Ref. [3]. We initially choose a rectangular region R such that all the KAM islands and cantori are contained in it (that is, R covers the mixing region). We then partition the x - y plane into n^2 rectangular cells, corresponding to the division of the x and the y axes into n equal segments. A given particle in an arbitrary position in R is considered to be located in the center of the corresponding cell. When a particle evolves in time through (13), this particle is mapped to another cell. If the mapping takes a particle outside the allowed region R , it escapes, and is discarded in the simulation. After advection, the particles undergo the reaction. We assume that all particles undergo a catalytic reaction, which acts as an infection: if a given cell

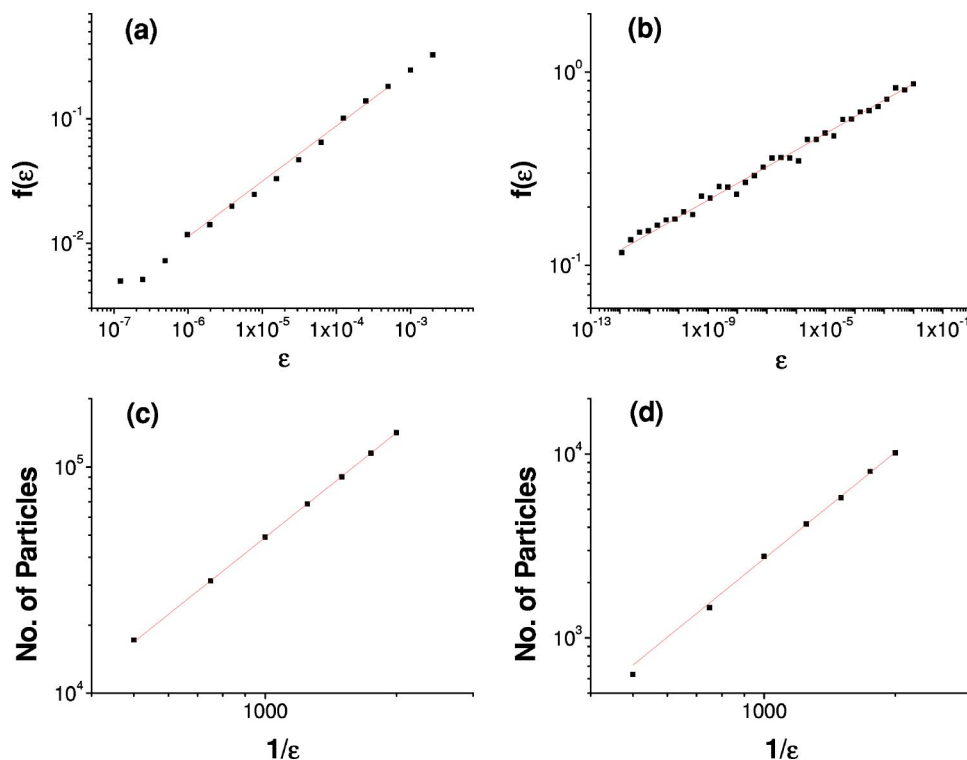


FIG. 3. (a) $f(\epsilon)$ outside the cantorus; the slope gives $d_{eff}=1.54\pm 0.01$. (b) $f(\epsilon)$ inside the first cantorus; $d_{eff}=1.915\pm 0.003$. (c) Number of reacting particles in the filamentary component of the equilibrium distribution as a function of the inverse of the grid size, for $\tau=1$; the slope gives directly $d_{ob}=1.53\pm 0.01$. (d) Same as (c), with $\tau=200$; $d_{ob}=1.92\pm 0.03$.

contains a particle before the reaction, all surrounding cells will also contain particles after the reaction. If an infected cell already has a particle, it remains unaltered. This is a coarse-grained approximation of the reaction front propagation, discussed in Sec. II. The complete dynamics of the system is thus composed of advection and reaction. This is clearly a discrete version of an autocatalytic process (1), where both space and time are discretized. We assume that condition (11) is satisfied, so that we do not have to concern ourselves with diffusion. To fully define the dynamics, we define the *reaction time* τ , which is the number of times we iterate the map (13) before applying the reaction. The reaction rate is given by $1/\tau$. The parameters in this discrete system are related to the reaction front velocity v by $v = \sigma/\tau$, where σ is the size of a cell. To recover the continuous dynamics, we go to the limit $n \rightarrow \infty$, $\sigma \rightarrow 0$, $\tau \rightarrow 0$, with $\sigma/\tau = v$ kept constant.

Using the above procedure, we simulate numerically the advection-reaction dynamics. We initially fix $\tau=1$. After an initial transient time, we find that the space distribution of the reacting particles settles down to an equilibrium that is independent of the initial conditions (except for those that lead to the empty equilibrium, corresponding to all particles escaping after a finite time). The equilibrium distribution is plotted in Fig. 2(b). This distribution represents a dynamical equilibrium, when particles are produced by the reaction at the same rate with which they escape through advection.

The equilibrium distribution of Fig. 2(b) is made up of two components: a bulky component B , which includes the region corresponding to the KAM islands and the outermost

cantorus [compare with Fig. 2(a)], and a filamentary component F , surrounding B [see Fig. 2(b)]. The existence of B is due to the presence of the KAM islands: if a particle is advected sufficiently near the boundary of an island, during the “infection” phase of the dynamics, one of the produced particles may be inside the island, and then, as the dynamics progresses, the whole island ends up being taken over by the particles. In fact, not only the islands are taken over, but, in our case, also their surrounding cantori. Although particles from within the cantori can escape, their typical escape time is much larger than the reaction time $\tau=1$ of Fig. 2(b). As a result, the number of particles inside the cantori increases faster than the loss caused by escape, and the cantorus seen in Fig. 2(a) becomes one single massive concentration of particles, where every cell is occupied, as shown in Fig. 2(b). In the case of a hyperbolic dynamics, there is no bulky region B . This is an important difference between the hyperbolic and nonhyperbolic cases.

For hyperbolic dynamics, the equilibrium distribution has a fractal structure (down to the grid size), with an observed fractal dimension d_{ob} equal to the dimension d of the unstable set in the underlying Hamiltonian dynamics [3]. Notice that the reaction introduces a minimum length $\epsilon = \sigma$, where σ is the grid size. This suggests that, for nonhyperbolic systems, the filamentary part F of the distribution must have an observed dimension d_{ob} equal to the effective dimension $d_{eff}(\epsilon)$ (with ϵ equal to the grid size), and not d . We have calculated the box-counting dimension of the distribution shown in Fig. 2(b), after excluding the bulky component. This is shown in Fig. 3(c) (squares). We have obtained

$d_{ob}=1.53\pm 0.01$, which is to within numerical error equal to $d_{eff}=1.54$, calculated previously for the region outside the first cantorus.

From the fact that d_{eff} depends on the location in phase space, we might expect the measured dimension d_{ob} of the equilibrium distribution to also depend on the location in the same way as d_{eff} , and to assume a greater value inside the cantorus. However, we have to take the reaction time τ into account: if τ is smaller than the typical escape time t_e inside the cantorus, empty cells created by escape will be immediately infected by neighboring particles, and the interior of the cantorus will always be a homogeneous block of particles, such as seen in Fig. 2(b). In this case, the effective dimension d_{eff} of this inner region does not manifest itself. If, on the other hand, $\tau \gtrsim t_e$, the reaction is not able to fill all the holes, and the distribution within a region of the cantorus becomes filamentary, with an observed dimension equal to d_{eff} . At the same time, since the escape time outside the cantorus is much smaller than inside, the equilibrium distribution outside the cantorus is depleted to almost nonexistence. From the above, we conclude that for $\tau \sim t_e$, the equilibrium distribution undergoes a structural transition, with regions that were formerly in the “bulky” zone becoming filamentary, and the observed dimension changing to a larger value. Because of the hierarchical organization of the cantori, this transition happens for an infinite number of values of τ , each transition corresponding to inner cantori, with larger escape times. In terms of the continuous dynamics, a region is expected to be bulky if $v \ll L/t_e$, where L is a characteristic (macroscopic) size. An increase in τ means a decrease in the reaction front velocity v .

To test our theory, we simulate the system’s dynamics for increasing values of τ . The result for $\tau=50$ and $\tau=200$ can be seen in Figs. 2(c) and 2(d). As τ is increased, the region outside the cantorus is depleted, and above a critical value τ_c , part of the region within the cantorus is “breached,” and becomes filamentary [Fig. 2(d)]. Comparing Fig. 2(d) and Fig. 2(b), the former’s structure does look more involved, suggesting a larger observed dimension. A box-counting cal-

ulation of d_{ob} confirms this [see Fig. 3(d)], and gives the result $d_{ob}=1.92$, in excellent agreement with $d_{eff}=1.91$, calculated previously for the nonreactive dynamics. Thus, our theory is supported by the simulations. Increasing τ further, we should in principle see other transitions, but the numerical limitations does not allow us to resolve them.

We note that for arbitrarily large τ , nonhyperbolic systems always have a nonempty equilibrium distribution, because the KAM islands correspond to $t_e=\infty$. This is another difference with hyperbolic systems, which always have a critical value of τ above which the system empties (the so-called *emptying transition* [3]).

VI. FINAL REMARKS

Summarizing our results, we have found that the dynamics of nonhyperbolic incompressible-flow advection-reaction systems is qualitatively very different from that of hyperbolic systems. In particular, the structure and observed dimension of the equilibrium distribution of reacting particles depend on both the lower length scale and on the reaction rate. The equilibrium distribution undergoes an infinite number of structural transitions as τ is increased (and v decreased), which are due to the presence of nested cantori in phase space. As a final remark, we note that if many reactions take place simultaneously in a flow (this is the case in the atmosphere, for instance), they may see different effective dimensions, depending on the values of the front velocity v (or, in the discrete dynamics, τ). Since different dimensions imply different production rates (see Ref. [3]), the dependence of d_{eff} on location may have important consequences for the production rates of competing chemical reactions (or biological processes).

ACKNOWLEDGMENTS

This research was funded by FAPESP and CNPq. We would like to thank Tamás Tél for many fruitful discussions.

-
- [1] E. Zemniak, C. Jung, and T. Tél, *Physica D* **36**, 123 (1994).
 - [2] J. C. Sommerer *et al.*, *Phys. Rev. Lett.* **77**, 5055 (1996).
 - [3] Z. Toroczkai *et al.*, *Phys. Rev. Lett.* **80**, 500 (1998); G. Károlyi *et al.*, *Phys. Rev. E* **59**, 5468 (1999).
 - [4] Z. Neufeld, C. López, and P. H. Haynes, *Phys. Rev. Lett.* **82**, 2606 (1999); Z. Neufeld *et al.*, *Phys. Rev. E* **61**, 3857 (2000).
 - [5] T. Tél, T. Nishikawa, A. Motter, and C. Grebogi, *Chaos* **14**, 72 (2004).
 - [6] I. R. Epstein, *Nature (London)* **374**, 321 (1995).
 - [7] G. Metcalfe and J. M. Ottino, *Phys. Rev. Lett.* **72**, 2875 (1994).
 - [8] J. D. Murray, *Mathematical Biology* (Springer, Berlin, 1993).
 - [9] J. Smoller, *Shock Waves and Reaction-diffusion Equations* (Springer, Berlin, 1983).
 - [10] G. K. Batchelor, *An Introduction to Fluid Dynamics* (Cambridge University Press, Cambridge, UK, 1967); D. J. Tritton, *Physical Fluid Dynamics* (Oxford University Press, Oxford, UK, 1988).
 - [11] T.-Y. Koh and B. Legras, *Chaos* **12**, 382 (2002).
 - [12] E. R. Abraham and M. M. Bowen, *Chaos* **12**, 373 (2002).
 - [13] Á Péntek, Z. Toroczkai, T. Tél, C. Grebogi, and J. A. Yorke, *Phys. Rev. E* **51**, 4076 (1995).
 - [14] T. Tél, in *Directions in Chaos*, edited by H. Bai-Lin (World Scientific, Singapore, 1996).
 - [15] D. G. H. Tan *et al.*, *J. Geophys. Res.* **103**, 1585 (1998); A. Mariotti *et al.*, *J. Atmos. Sci.* **57**, 402 (2000).
 - [16] G. Károlyi *et al.*, *Proc. Natl. Acad. Sci. U.S.A.* **97**, 13661 (2000).
 - [17] G. Károlyi, I. Scheuring, and T. Czárán, *Chaos* **12**, 460 (2002).
 - [18] Y.-T. Lau *et al.*, *Phys. Rev. Lett.* **66**, 978 (1991).
 - [19] R. A. Fischer, *Ann. Eugenics* **7**, 353 (1937).
 - [20] A. Kolmogorov, I. Petrovsky, and N. Piscounoff, Moscow

- Univ. Bull. Math. **1**, 1 (1937).
- [21] V. I. Arnold, *Mathematical Methods of Classical Mechanics* (Springer, New York, 1986).
- [22] The concept of effective dimension was used before in A. E. Motter, Y.-C. Lai, and C. Grebogi, Phys. Rev. E **68**, 056307 (2003).
- [23] M. Hénon, Q. Appl. Math. **27**, 291 (1969); A. J. Dragt and J. M. Finn, J. Math. Phys. **17**, 2215 (1976).
- [24] C. Grebogi *et al.*, Phys. Lett. **99A**, 415 (1983).
- [25] K. J. Falconer, *The Geometry of Fractal Sets* (Cambridge University Press, Cambridge, UK, 1985).
- [26] We notice that d_{eff} is only well-defined if the plot of $\ln f$ versus $\ln \epsilon$ is approximately a straight line for a wide range of scales. This is true in the case of the map (13), and also in most other nonhyperbolic systems.
- [27] T. Tél, G. Károlyi, A. Péntek, I. Scheuring, Z. Toroczkai, C. Grebogi, and J. Kadtke, Chaos **10**, 89 (2000).